doi:10.1111/evo.13127

Repeated intraspecific divergence in life span and aging of African annual fishes along an aridity gradient

Radim Blažek,[1] Matej Polačik,[1] Petr Kačer,[2] Alessandro Cellerino,[3,4] Radomil Řežucha,[1] Caroline Methling,[1] Oldřich Tomášek,[1,5] Kamila Syslová,[2] Eva Terzibasi Tozzini,[3] Tomáš Albrecht,[1,5] Milan Vrtílek,[1] and Martin Reichard[1,6]

[1]*Institute of Vertebrate Biology, Academy of Sciences of the Czech Republic, Květná 8, 603 65 Brno, Czech Republic*

[2]*Laboratory of Medicinal Diagnostics, Department of Organic Technology, University of Chemistry and Technology, Technická 5, 166 28 Prague, Czech Republic*

[3]*Bio@SNS, Scuola Normale Superiore, Department of Neurosciences, Piazza dei Cavalieri 7, 56126 Pisa, Italy*

[4]*Fritz Lipmann Institute for Age Research, Leibniz Institute, Beutenbergstr. 11, D-07745 Jena, Germany*

[5]*Department of Zoology, Faculty of Sciences, Charles University in Prague, Viničná 7, 128 44 Praha, Czech Republic*

[6]*E-mail: reichard@ivb.cz*

Received June 7, 2016
Accepted November 9, 2016

Life span and aging are substantially modified by natural selection. Across species, higher extrinsic (environmentally related) mortality (and hence shorter life expectancy) selects for the evolution of more rapid aging. However, among populations within species, high extrinsic mortality can lead to extended life span and slower aging as a consequence of condition-dependent survival. Using within-species contrasts of eight natural populations of *Nothobranchius* fishes in common garden experiments, we demonstrate that populations originating from dry regions (with short life expectancy) had shorter intrinsic life spans and a greater increase in mortality with age, more pronounced cellular and physiological deterioration (oxidative damage, tumor load), and a faster decline in fertility than populations from wetter regions. This parallel intraspecific divergence in life span and aging was not associated with divergence in early life history (rapid growth, maturation) or pace-of-life syndrome (high metabolic rates, active behavior). Variability across four study species suggests that a combination of different aging and life-history traits conformed with or contradicted the predictions for each species. These findings demonstrate that variation in life span and functional decline among natural populations are linked, genetically underpinned, and can evolve relatively rapidly.

KEY WORDS: **Intraspecific variation, life span, neoplasia, pace-of-life syndrome, parallel evolution, reproductive senescence.**

Aging is a complex process leading to an increase in mortality risk with age due to a decline in vital functions. Functionally, aging is associated with degradation at systemic, cellular, and molecular levels (López-Otín et al. 2013). Demographically, aging is expressed as an increase in the probability of death with chronological age above the baseline mortality risk (Pletcher et al. 2000). The evolution of aging rate is ascribed to trade-offs in response to patterns of adult extrinsic (i.e., environmentally driven) mortality (Medawar 1952; Williams 1957), with aging arising as a by-product of selection to maximize reproduction (Kirkwood 1977). Under higher extrinsic mortality, earlier and greater investment in reproduction is favored over investment in self-maintenance, resulting in the evolution of steeper aging rates (Kirkwood and Austad 2000) and a suite of life-history traits related to rapid reproduction (Stearns 1992). This theory is empirically supported by broad-scale comparative studies (reviewed in Ricklef 2010), experimental work on closely related species (Tatar et al. 1997; Dudycha and Tessier 1999),

EVOLUTION
INTERNATIONAL JOURNAL OF ORGANIC EVOLUTION

and from experimental evolution within species (reviewed in Rose 1994).

Variation in life span within a species can be substantial (Rose 1994; Lohr et al. 2014). Standing genetic variation for life span and aging frequently responds to artificial selection (Rose 1994; Stearns et al. 2000; Chen and Maklakov 2012; Kraus et al. 2013), though life span differences are often derived from variation in baseline mortality rather than from differential increase in mortality risk with age (Pletcher et al. 2000; Ricklefs 2010). This observation pertains even to the differences between captive and wild populations (Bronikowski et al. 2002; Ricklefs 2010) and the rate of increase in mortality risk with age appears relatively conserved within species and among closely related species (Ricklefs 2010).

Recent empirical and theoretical studies suggest that, within species, high condition-dependent extrinsic mortality can be selected for extended rather than reduced life span due to a positive association between individual condition and survival (Williams and Day 2003; Chen and Maklakov 2012; Maklakov et al. 2015). These observations translate into life span differences among populations, suggesting that the aging patterns within species can evolve in the opposite direction to the pattern among species (Reznick et al. 2004; Williams et al. 2006). Current evidence for a primary role of condition dependence comes from experimental selection on *Caenorhabditis remanei* subjected to a heat-shock (Chen and Maklakov 2012) and a common garden experiment with natural populations of the guppy fish (*Poecilia reticulata*; Reznick et al. 2004) from habitats with contrasting predation rates. In these studies, however, the strength and contrast in condition-dependent mortality risk (i.e., the source of selection on life span and aging) were substantial. Given that earlier studies on natural populations (Austad 1993) conformed to predictions of the classic evolutionary theory of aging, it remains to be investigated how widespread is the reversed pattern of aging among natural populations.

Linking data on actuarial aging and functional deterioration is challenging but essential to understand the evolution of aging in natural populations (Fontana et al. 2014). Functional declines associated with aging are diverse (López-Otín et al. 2013) and may or may not be correlated (Massot et al. 2011; Hayward et al. 2013). Oxidative stress, that is, cellular damage by reactive oxygen and nitrogen species (RONS) arising from metabolic and immune processes, is known to be associated with age-related functional declines and neoplasia (Reuter et al. 2010; López-Otín et al. 2013). Lower RONS formation and/or higher resistance of cellular components to oxidative damage correlates with elevated longevity (Monaghan et al. 2009; Pamplona and Costantini 2011). Neoplasia represent a serious functional decline associated with aging in vertebrates, including fishes (Kishi et al. 2003), and is associated with other functional declines (di Cicco et al. 2011; Baumgart et al. 2015). Decrease in reproductive success is another important source of decline in individual fitness contributing to aging, with recognized differences among species (Bouwhuis et al. 2012; Jones et al. 2008) and the potential for variation among populations of a species. Different aspects of reproductive senescence (e.g., reproductive allotment, clutch size, fertilization success, egg size) may vary greatly in their expression (Hayward et al. 2015) and hence in their contribution to overall reproductive senescence.

Life span and aging coevolve with other life-history traits. Short life span is predicted to be associated with early sexual maturity that may be achieved by maturation at a smaller size, more rapid juvenile growth, or larger neonate size (Stearns 1992). The physiological and behavioral components of life history can be integrated into a so-called "pace-of-life syndrome" (Ricklefs and Wikelski 2002), where rapid life history (short life span, rapid maturation) is associated with high metabolic rates (Wikelski et al. 2003) and more active, aggressive, and bold behavior (Réale et al. 2010).

Here, we use replicated populations of four species of African annual killifish to test the effects of extrinsic mortality on the evolution of aging at demographic, cellular, structural, and reproductive levels, along with their life-history trade-offs and consequences. *Nothobranchius* killifishes are ideal for investigating the evolutionary trajectory of aging. They inhabit temporary savannah pools and have evolved naturally short life spans as a response to the seasonal desiccation of their habitat (Cellerino et al. 2016). In the rainy season, the fish hatch from desiccation-resistant eggs and achieve sexual maturity in a few weeks (Blažek et al. 2013). Adult fish live only a few months. In the wild, their maximum life span is limited by pool desiccation, which varies across a gradient of aridity (Terzibasi Tozzini et al. 2013). The short life span of *Nothobranchius* is retained in captivity when fish are shielded from extrinsic mortality and varies among species (Terzibasi Tozzini et al. 2013). Importantly, their life span is temporally condensed rather than prematurely terminated and is associated with a range of measurable functional declines (Di Cicco et al. 2011; Cellerino et al. 2016).

We used within-species contrasts in life span expectancy (dry- and wet-region populations that vary in the duration of their ephemeral habitats) to conduct experiments in a common garden environment using F1 generations of natural populations of four *Nothobranchius* species (Table 1). We predicted fish from dry-region populations (that inhabit areas with a short rainy period) to live intrinsically shorter lives and age more steeply in terms of increase in mortality risk and decline in functional and reproductive traits with age. We further predicted larger offspring size; more rapid maturation; higher investment in reproduction; more active, bolder, and aggressive behavior; and higher metabolic rates in fish from dry-region populations.

Table 1. Overview of study populations and their origin.

Species	Region	Prec[1]	N^2	Collection code MZCS	River basin	GPS coordinates	Altitude (m)	Aridity index[3]	Species presence[4]	Founders[5]
N. furzeri	Dry	560	102	NF222	Chefu	S21.873 E32.801	158	0.3082	O, P, F	20 + 40
N. furzeri	Wet	621	99	NF121	Limpopo	S24.358 E32.974	30	0.3426	O, F	15 + 28
N. kadleci	Dry	851	108	NK91	Gorongosa	S20.688 E34.106	64	0.5114	O, K	10 + 20
N. kadleci	Wet	939	101	NK430	Pungwe	S19.281 E34.221	52	0.5051	O, K	10 + 21
N. orthonotus	Dry	573	131	NO2	Limpopo	S24.064 E32.732	79	0.3203	O, P, F	6 + 22
N. orthonotus	Wet	1269	139	NO528	Pungwe	S19.697 E34.783	38	0.8115	O, P	16 + 26
N. pienaari	Dry	490	140	NP505	Limpopo	S23.530 E32.578	129	0.2735	O, P, F	10 + 22
N. pienaari	Wet	1275	157	NP514	Pungwe	S19.700 E34.785	36	0.8179	O, P	15 + 27

[1]Annual precipitation in millimeter, data from WorldClim—Global Climate Data: www.worldclim.org.
[2]Number of experimental fish, including fish censored for functional decline analyses.
[3]Data from CGIAR Consortium for Spatial Information: www.cgiar-csi.org/Aridity.
[4]Presence of *N. orthonotus* (O), *N. furzeri* (F), *N. kadleci* (K), and *N. piennari* (P) at the site.
[5]The number of males + females imported to the laboratory to produce F1 generations used in the experiment.

Materials and Methods

STUDY AREA, ARIDITY GRADIENT, AND EXPERIMENTAL POPULATIONS

All study species inhabit southern and central Mozambique, where a steep cline of aridity is generated by a decrease in precipitation with increasing distance from the coast and with increasing latitude (Fig. S1). We imported dry- and wet-region populations for each species, representing populations with short and long life expectancy (Table 1). We targeted study populations that unambiguously belonged to well-separated clades associated with dry or wet regions of the species range. Hence, dry- and wet-region populations came from different population-genetic groups and had sufficient time to evolve to different life-history optima. Dispersal between *Nothobranchius* populations is minimal and there is no recent introgression between the clades (Bartáková et al. 2013, 2015). To confirm that local conditions did not override the climatically driven environmental setting, we recorded the state of each pool (wet/dry phase) during six expeditions to the study area (2011–2015; February to July). Only pools suitable for *Nothobranchius* were screened (based on experience from four previous expeditions from 2008 to 2010). Pools that occurred within a range of population-genetic groups from which the source population was collected (Bartáková et al. 2015) were contrasted between dry and wet regions for each species using a generalized linear mixed model (GLMM, *lme4* package; Bates et al. 2014) with binomial error distribution (fixed effect: *region*; random effects: *species* and *expedition*). Pools in dry-region sites were significantly drier ($z = 6.38$, $P < 0.001$, $n = 48$), with large contrasts between populations of *Nothobranchius orthonotus*, *Nothobranchius pienaari* and *Nothobranchius furzeri* (all $z > 3.5$, $P < 0.001$) and nonsignificant contrast between populations of *Nothobranchius kadleci* ($z = 1.51$, $P = 0.131$).

Experimental fish were F1 descendants of wild parents. Eggs from the first two months after import were discarded to minimize environmentally driven maternal effects; *Nothobranchius* are extreme income breeders and repeatedly replace their oocyte stock during a two-month breeding period under standardized conditions (Vrtílek and Reichard 2015). Eggs were stored in an incubator (Pollab, Q-CELL 60–240) at 23.5–24.5°C for at least 16 weeks following standard methods (Polačik et al. 2016), ensuring that all embryos developed via diapause. Experimental fish were hatched simultaneously by watering the incubation substrate with dechlorinated tap water (16°C). More than 500 juveniles hatched in each population. The experiment consisted of two phases. The first set of four populations (*N. furzeri*, *N. kadleci*) was hatched on 7 September 2011 (last fish died in December 2012); the second set (*N. orthonotus*, *N. pienaari*) was hatched on 22 May 2013 (last fish died in March 2015); it was not logistically possible to study all eight populations simultaneously.

Note that contrasts were studied within species (between dry- and wet-region populations), therefore the comparisons were employed on fish held under strict standardized common conditions. Experimental conditions were equally suitable for all study populations regardless of their origin; aridity gradient is associated with persistence of natural pools, but not with other environmental or biotic differences (Reichard et al. 2009; Polačik et al. 2011; Terzibasi Tozzini et al. 2013; Reichard et al. 2014).

From the age of two days (*N. furzeri*, *N. kadleci*), four days (*N. orthonotus*), or 10 days (*N. pienaari*) (depending on size of the juveniles), fish were housed in social groups in a set of 24 L aquaria. Dead juveniles were replaced with fish of the same age and housing density history from spare stock tanks. After reaching a size for individual marking (*N. orthonotus*: six weeks, *N. furzeri*, *N. kadleci*: seven weeks), fish were briefly anesthetized and a single visible implant elastomer tag (Northwestern Marine Technology, USA) was applied subcutaneously. The small size of *N. pienaari* precluded marking. Twelve aquaria were used for each population. Initial adult density was 12 fish per tank, except for *N. orthonotus* (the largest species), where density was 10 fish per tank. Tanks were equipped with air-driven sponge filters and 25–30% of water was exchanged two to three times each week. Fish were kept under a 12-h light:12-h dark regime in aged tap water (conductivity 550 $\mu S/cm^2$, temperature 26 ± 2°C). For the first 30 days, all fish were fed twice each day to satiation and once each day thereafter. Fish were initially fed with live *Artemia* nauplii and their diet was supplemented with chopped bloodworm (*Chironomus* larvae) and *Tubifex* from the age of 10 days (*N. orthonotus*), 13 days (*N. kadleci*, *N. furzeri*), or 22 days (*N. pienaari*). *Artemia* feeding was discontinued at age 30 days. *Tubifex* were not used for feeding *N. furzeri* and *N. kadleci*. All tanks received the same ration (approximately 15% of body mass of the fish in the tank). Aquaria were monitored daily and any dead fish were recorded and removed.

SURVIVAL AND ACTUARIAL AGING

Mortality hazard was analyzed using linear effects Cox proportional hazards models (*coxme* package) (Therneau 2015a) with *region* as the fixed factor and *population* nested within *species* as random factors. Species-specific datasets were also tested (Cox proportional hazards models; *survival* package) (Therneau 2015b) to provide within-species contrasts in mortality hazards between dry- and wet-region populations.

Population-specific survival trajectories were compared using Bayesian survival trajectory analysis (BaSTA) (Colchero et al. 2012). First, we fitted three basic models (Weibull, Gompertz, Logistic), each with three-shape parameters (simple, Makeham, Siler/bathtub) to population-specific data. Exponential mortality models were included as the null models. The exponential model has a single parameter describing baseline mortality rate that is constant across life span. The Gompertz model combines baseline mortality (initial mortality rate, IMR), with the γ (gamma) parameter that describes an increase in mortality with age (rate of aging, RoA). The logistic model is the population-level solution to the Gompertz model where an additional parameter s accounts for the variance in frailty (i.e., the dispersion on individual heterogeneity) (Vaupel and Yashin 1985). The Weibull model combines *IMR* and *RoA* in additive form (i.e., independent, assuming primarily intrinsic causes of death at advanced age), whereas the Gompertz-family models combine *IMR* and *RoA* in multiplicative form (assuming increase in vulnerability to extrinsic mortality with age) (Pletcher et al. 2000). The shape parameters captured age-independent mortality (Makeham term) (Pletcher 1999; Pletcher et al. 2000) and initially higher mortality in young adults (Siler "bathtub shape" modification with a declining Gompertz function) (Colchero et al. 2012). We compared model fits using deviance information criterion (DIC). Individuals removed for functional decline analyses were deleted from this dataset because the BaSTA algorithm would incorrectly assume that censored individuals died shortly after their removal given a high apparent recapture rate in the data matrix. We used four runs of each model, each with 150,000 MCMC iterations, burn-in of 15,001, and thinning by sampling every 50th estimate. We set the minimum age to estimate parameters to the age when all individuals of a given species were sexually mature (five weeks in *N. orthonotus*, six weeks in *N. furzeri* and *N. kadleci*, eight weeks in *N. pienaari*). Using population-specific rankings of the models (Table S1), we chose the best model for each species. The best models were run with 450,000 MCMC (Monte Carlo Markov Chain) iterations, burn in of 45,001 and thinning by sampling every 200th estimate to provide a posterior distribution of parameters for each population. Model parameters were compared using Kullback–Leibler discrepancy criterion (KLDC). The KLDC varies between 0.5 (complete overlap) to 1.0 (no overlap) and is sometimes approximated to frequentist P values as KLDC $>$ 0.65 comparable to $P < 0.05$ for difference between the treatment groups (Larson et al. 2016). We also combined all eight populations in a single analysis.

ANALYTICAL APPROACH TO FUNCTIONAL AND REPRODUCTIVE AGING

We recorded a set of phenotypic traits (oxidative stress, histopathology, reproductive allotment) that were predicted to suffer from functional deterioration at two time points—early and late in life. These estimates of functional and reproductive aging required removal of individuals from the study cohort and they were censored from the survival analysis at the age of their removal. The exact age for functional analyses was a compromise between exact chronological age and proportional mortality across all study populations (Table S2). We prioritized matching

absolute age across populations over matching proportional mortality, inevitably resulting in sampling late-life samples before 50% mortality had been reached in the longest lived population. Nevertheless, young fish (12–14 weeks old) were typically sampled in the first quartile and old fish (23–30 weeks old) in the third quartile of their population-level life spans.

Data were analyzed using general mixed effect models (LMM) and GLMM in *lme4* package (Bates et al. 2014) for Gaussian, Poisson, negative binomial, and binomial distributions, with *region* (dry, wet), *age* (young, old) and their interaction as the fixed factors of interest. We predicted higher and more rapid (*region* × *age* interaction) deterioration in the dry region. Because we only tested fish from a single population of each species from each region but were primarily interested in interregional differences, we included the random effect of *population* nested within *species* in all analyses to avoid pseudoreplication by concluding regional level inferences from population-specific data. Whenever appropriate, we also included covariates (*body size* and *body mass*) and additional fixed effects (*sex*). We first constructed the full model, including all fixed effects and covariates. Nonsignificant covariates and additional fixed effects were removed from final models. *age* and *region* effects were always retained. A nonsignificant *age* × *region* interaction was removed from final models to obtain unbiased factor estimates. Because analysis with and without body length (or body mass) as a covariate could have a different biological interpretation, we provide both results wherever appropriate. Model assumptions were checked by plotting residuals against fitted values. Overdispersion was detected in the analysis of the number of eggs and a negative binomial distribution was used instead of Poisson distribution to control for it. The analyses of clutch size, fertilization rate, and egg size were nondestructive and were repeated at 10 weeks intervals. To account for nonindependence of records taken from the same individuals, *female ID* was included as an additional random effect in the particular LMM analyses. In *N. pienaari* (not individually marked), aquarium ID was used instead of female ID.

We also provide species-specific analyses of all traits. Species-specific analyses were general (and generalized) linear models (LM, GLM) except in the case of reproductive traits where random effects related to individual female IDs were present and LMM and GLMM were used (*lme4* package).

REPRODUCTIVE TRAITS

Relative ovary mass was measured at two age points (Table S4), using a total of 164 females. Adult *Nothobranchius* reproduce daily. A random subsample of females was separated from males overnight to standardize their reproductive status (*Nothobranchius* ovulate their daily batch of eggs overnight) (Polačik et al. 2016). In the morning, females were killed with an overdose of anesthesia and dissected. Total length (TL, from the tip of the snout to the end of the caudal fin) and total wet mass (Wt) were recorded, ovaries dissected, and their mass (Wg) and the mass of the eviscerated body (all internal organs removed) (We) were weighed to the nearest 0.0001 g. The gonadosomatic index was calculated for each female (GSIe = [Wg/We] × 100 and GSIt = [Wg/Wt] × 100) (Wootton and Smith 2015). Statistical analyses were performed using GSIe, GSIt, and raw Wg (Wt used as covariate). We report data on GSIt (gonadosomatic index calculated using total wet mass), but all results were qualitatively identical.

A subset of fish was tested every 10 weeks for egg production (clutch size) and fertilization rate. Females were isolated in 2 L aquaria prior to experimental spawning to standardize their egg reserves. After 24 h, a male from the same population was added and fish spawned for 2 h. This design ensured that females laid all their ovulated eggs (Polačik and Reichard 2011). Aquaria had a layer of fine sand as a spawning substrate. Eggs were counted and their fertilization status (fertilized, nonfertilized) recorded after 18–24 h (Polačik et al. 2016). We measured egg diameter from a total of 364 clutches (subsets of up to 10 eggs per clutch). Given a trade-off between egg size and number (Vrtílek and Reichard 2016), we included egg number as a covariate in the analysis of egg size.

OXIDATIVE STRESS

Biomarkers of oxidative stress were analyzed in 151 individuals. Fish were sacrificed and brain, liver, and heart were stored immediately in liquid nitrogen. Following each tissue homogenization in acetonitrile with deuterium-labeled internal standards, oxidation products of nucleic acids (8-hydroxy-2′-deoxyguanosine [8-OHdG]; 8-hydroxyguanosine [8-OHG]), proteins (o-tyrosine, 3-nitrotyrosine, 3-chlorotyrosine), and lipids (8-isoprostane) were determined by high-performance liquid chromatography–electrospray ionization–high-resolution mass spectrometry (HPLC–ESI–HRMS) using LTQ Orbitrap Velos coupled with Accela 600 Pump, Accela AS autosampler (all Thermo Scientific, Waltham, MA, USA) and Gemini NX-C18 column (Phenomenex, Torrance, CA, USA) (Syslová et al. 2014). Full analytical details are given in Table S3. Tissues from experimental fish were analyzed for *N. orthonotus* and *N. pienaari*, but a new cohort of fish was produced to collect *N. furzeri* and *N. kadleci* tissue, because HPLC–ESI–HRMS analysis was not available to us when *N. furzeri* and *N. kadleci* were followed. The procedure for raising *N. furzeri* and *N. kadleci* for oxidative stress analysis was identical to experimental fish. MZCS NF002 population (collection GPS: S24.06347 E32.73220, altitude 79 m, seven male and 10 female founders) was used instead of population MZCS NF121 for wet-region *N. furzeri*. Population MZCS NF002 comes from a pool located 41 km from MZCS NF121 and the two populations are genetically closely related (Bartáková et al. 2013). We combined data across organs and biomarkers

using principal component analysis and used PC1 as a representation of oxidative stress (Table S6). Additionally, organ- and biomarker-specific analyses were performed.

HISTOPATHOLOGY

The presence and severity of liver and kidney tumors and cephalic kidney swelling (an indicator of dysfunction due to swelling and clogging of the renal tubules) (Di Cicco et al. 2011) were analyzed in *N. furzeri* and *N. kadleci*. Fish were sacrificed and dissected. The macroscopic swelling of the cephalic kidney was visually scored during dissection (score 0: no swelling, score 4: swollen to 10 times normal organ size). Liver and cephalic kidney were preserved in Baker's solution, embedded in Paraplast, sectioned (5 μm) and stained in H&E. Tumors (hepatomas, hepatocarcinomas, and renal carcinomas) were scored using a five-grade pathological scale (Di Cicco et al. 2011) (score 0–4, 0: no tumor, 4: >50% of tissue filled with tumors). Visual examples of tumors and tumor-associated tissue pathology are illustrated in Figure S2.

LIFE-HISTORY TRAITS

Traits were compared between dry- and wet-region populations and analyzed by LMMs and GLMMs as for functional aging analyses, except that data were collected at a single time point (no fixed effect *age*); at the age of 11–20 weeks at 10–50% mortality at the population level.

Body size at hatching was measured by sacrificing a subset of fish immediately upon hatching, storing in 4% formaldehyde and measuring their TL under a binocular microscope. All other TL measurements were completed by photographing live fish from above in shallow water in containers with a reference scale. TL was measured from photographs using ImageJ software. Fish were measured at regular intervals (weekly until the age of six weeks, every two weeks until the age of 14 weeks, and monthly thereafter). The largest female and male in the aquaria were additionally measured on the day of first production of fertilized eggs to estimate size at sexual maturity. Maximum size was the last measurement before death (Polačik et al. 2014a).

Sexual maturity was scored as the first production of fertilized eggs. Social aquaria were provided with a glass bowl filled with a layer (1.5 cm) of fine black sand (grain diameter 1-1.5 mm) and bowls were checked daily for the presence of eggs. Eggs were collected and checked for fertilization. This provided one replicate for each tank.

Routine metabolic rate (RMR) and maximum oxygen consumption (MO_2max) was recorded for 66 individuals from dry and wet populations of *N. pienaari* and *N. orthonotus* at the age of 19–20 weeks. RMR and MO_2max were quantified by computerized intermittent flow-through respirometry (Steffensen 1989) using a static respirometry system (Loligo Systems, Tjeldboden, Denmark). The protocol included an initial 3 min chasing followed by 30 sec air exposure (to estimate MO_2max). Fish were then placed in a 55 mL (90 mL for large fish) chamber submerged in a 10 L outer tank supplied with water from a reservoir, maintained at 24 ± 0.1°C. Chamber oxygen partial pressure (pO_2) was measured with an OXY–4mini (PreSens, Regensburg, Germany) fiber optic O_2 transmitter and recorded with AutoResp4^{TM} software. Mass-specific oxygen consumption (MO_2) was derived from the decrease in chamber pO_2 during a 5 min measuring period. Chambers were periodically flushed for 4 min. followed by a closed 1 min wait period. MO_2max was determined as the first MO_2 measurement after the fish was placed in the chamber. MO_2 measurements during the following 24 h were used to estimate RMR (Steffensen 1989). Metabolic scope (MS) was quantified as MS = MO_2max – RMR. All measurements were corrected for microbial respiration. *Sex* was an additional fixed factor and *wet mass* was covariate in the analyses as metabolic rate scales with body mass (Clarke and Johnston 1999).

Exploratory behavior was scored in a shallow opaque plastic aquarium (450 × 350 mm^2, water depth 25 mm) with a reference grid (25 × 25 mm^2) drawn on the bottom. The test aquarium was situated in the same room as the social aquaria. Water was taken from social tanks. Fish were fed ad libitum before and between trials to standardize their satiation and metabolic activity. Fish (tested individually) were transferred into the test tank and after 1 min acclimatization, their movement was monitored using a camera mounted above the tank for 4 min. Light conditions were standardized by the use of an external dimmed lamp. For *N. furzeri* and *N. kadleci*, fish movement was analyzed by replaying videos in JWatcher 1.061 (Blumstein and Daniel 2007) by scoring the number of grids crossed during a 4 min period. For *N. orthonotus* and *N. pienaari*, recording conditions were identical except that no grid was drawn on the aquarium bottom. Instead, a ruler provided scale for software calibration. Videos of *N. orthonotus* and *N. pienaari* were analyzed by Tracker 4.82 (Brown 2009) using absolute distance traveled by individuals during 4 min. *Nothobranchius furzeri* and *N. kadleci* fish were not reanalyzed by Tracker software because the bottom grid was not compatible with automated fish tracking.

Boldness was scored as time taken to leave a refuge in a novel environment in a design similar to Brown and Braithwaite (2004). Experimental conditions (water quality, satiation, lighting) matched exploratory behavior analysis, but fish were individually positioned in an opaque plastic container (80 mm length × 150 mm width × 160 mm height) with a sliding door, positioned at one side of the test aquarium (550 × 490 mm). The test aquarium was filled with water to a depth of 80 mm and had three sides covered by opaque foil to prevent any external disturbance. After 2 min, the sliding door was lifted and the fish allowed to leave the container. The time taken to depart the refuge (Time 1:

tip of snout outside refuge, Time 2: entire body outside refuge) was measured. Fish that did not leave the refuge within 10 min (60 out of 313 fish) were censored at 10 min (mixed effect Cox regression). Analyses for Time 1 and Time 2 were congruent; only Time 2 is reported.

Male–male aggression is a common feature of *Nothobranchius* behavior and positively correlates with access to females (Polačik and Reichard 2009). Male aggression (only in *N. furzeri* and *N. kadleci*) was scored as the number of attacks by the focal fish against a size-matched male from the same population held in a 1 L glass jar positioned in the middle of the experimental aquarium (43 L, 160 mm depth) during a 15-min period. All other conditions were identical to the analysis of other behavioral traits.

Results

SURVIVAL AND ACTUARIAL AGING

Across species, dry-region populations had a 32.9% higher mortality hazard than wet-region populations (mixed-effect Cox model: $z = 2.28$, $P = 0.023$). In within-species contrasts, the largest difference was detected between the populations of *N. pienaari* (60%, $P < 0.001$) and *N. furzeri* (35%, $P = 0.011$), with a marginal difference in *N. kadleci* (26%, $P = 0.075$) and no difference in *N. orthonotus* (−3%, $P = 0.820$). Median and maximum (∼90% quantile) life span matched survival patterns (Fig. 1).

Modeling age-specific survival and mortality patterns in BaSTA revealed an increase in mortality with age in all populations. The logistic model provided the best explanation of aging patterns in the populations of the shortest lived species (*N. furzeri*) and demonstrated presence of late-life mortality plateaus in populations of this species. A Weibull model (which can also integrate population-level deceleration in *RoA* with advancing age) was the best-fitting model for the other three species, with a bathtub shape (i.e., Siler model) for the mortality curve in *N. pienaari* where early adult mortality was high in a dry-region population (Fig. 1). A significantly faster increase in mortality with age (*RoA*, KLDC > 0.65) was demonstrated in dry-region populations of all study species, except for *N. orthonotus* (Table 2 and Fig. S3). Combining all eight populations into one dataset showed the logistic model to be the best fit and this model provided a concordant interpretation of the patterns and variability in aging among populations (Table S5 and Fig. S4).

FUNCTIONAL AGING

The composite measure of oxidative stress (PC1: Table S4) in dry-region populations had higher values overall (LMM: region: $t_{3.74} = 3.17$, $P = 0.037$) and exhibited a steeper increase with age (age: $t_{141.43} = 30.12$, $P < 0.001$; interaction: $t_{141.28} = 5.85$, $P < 0.001$) than in wet-region populations (Fig. 2A). The pattern was consistent across oxidative damage to lipids (8-isoprostane), proteins (o-tyrosine), and DNA (8-OHdG) in all three tissues (heart, brain, and liver). Differences between dry- and wet-region populations were robust across all tissues, whereas age-related decline was relatively weaker in brain tissue (Table S6). The outcome was also consistent across species, though the interaction term (i.e., steeper increase in oxidative stress in dry-region populations) was marginally nonsignificant in *N. furzeri* and *N. kadleci* (Fig. 2A and Table S7).

Across species, tumor-related histopathologies in liver and kidney were higher in dry-region populations and kidney pathologies increased with age. Macroscopic analysis of tumor-related cephalic kidney swelling demonstrated higher scores in old fish (Poisson GLMM: $z = 4.21$, $P < 0.001$, $n = 79$) and in dry-region populations ($z = 2.87$, $P = 0.004$), though not a significantly steeper increase with age in dry-region populations ($z = 0.37$, $P = 0.710$; Fig. 2B). Kidney swelling scores also increased with fish TL ($z = 4.37$, $P < 0.001$). The scores of kidney swelling and renal tumors were positively correlated (Spearman: $r_{79} = 0.32$, $P = 0.007$). Histopathological analysis of cephalic kidney demonstrated that fish from dry-region populations had higher renal tumor load (Poisson GLMM: $z = 2.04$, $P = 0.042$, $n = 72$) but its increase with age was not significant ($z = 1.49$, $P = 0.137$) in either region (interaction: $z = 0.88$, $P = 0.379$; Fig. 2C). Concordant results were found for tumor load in liver, with much higher liver tumor scores in fish from dry-region populations (Poisson GLMM: $z = 8.68$, $P < 0.001$, $n = 78$), but no increase with age ($z = 0.08$, $P = 0.938$) in any region (interaction: $z = 0.71$, $P = 0.478$; Fig. 2D). The same results were repeated in species-specific analyses (Fig. 2B–D; Table S7).

REPRODUCTIVE AGING

Reproductive allocation (measured as relative ovary mass) did not differ between dry and wet regions (LMM: $t_{3.1} = 0.14$, $P = 0.895$), but was generally higher in old females ($t_{155.3} = 3.94$, $P < 0.001$). The effect of age on reproductive allocation lost statistical significance after controlling for differences in TL (age: $t_{133.1} = 1.88$, $P = 0.063$; TL: $t_{80.2} = 1.36$, $P = 0.176$). Species-specific data demonstrated higher relative gonad mass in older *N. kadleci* and *N. pienaari* females, but not in the other two species (Fig. 3A, Table S8).

Total number of eggs in a clutch decreased with age in the dry-region populations but tended to increase in the wet-region populations (negative binomial GLMM, age: $z = 2.70$, $P = 0.007$; region: $z = 1.89$, $P = 0.059$; interaction: $z = 3.86$, $P < 0.001$, $n = 790$; Fig. 3B). A steep decline in relative clutch size ($z = 15.87$, $P < 0.001$; Fig. 3C) was evident after accounting for total female size as a highly significant covariate ($z = 21.31$, $P < 0.001$). The relative clutch size tended to be larger in dry regions ($z = 1.76$,

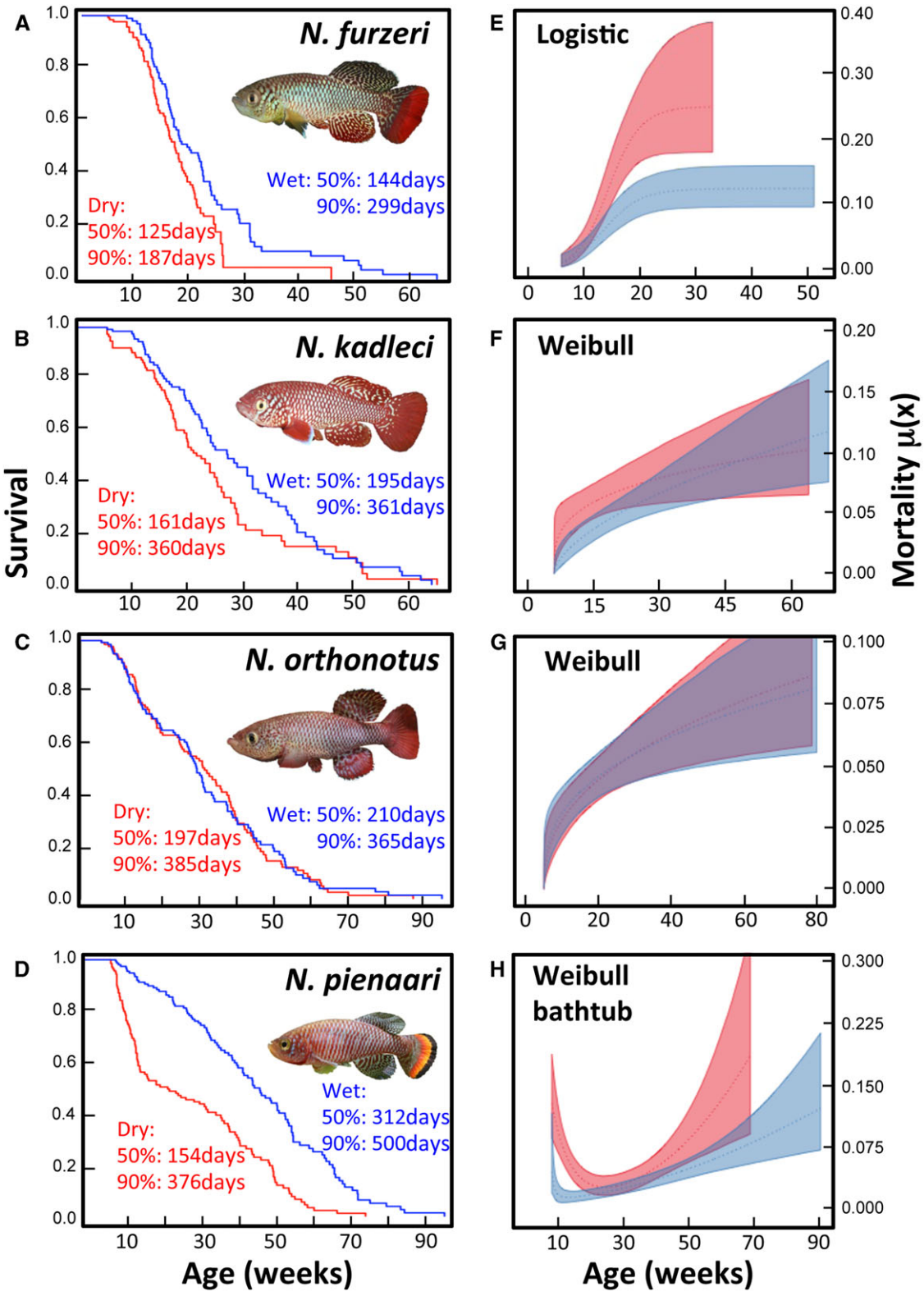

Figure 1. Population-specific survivorship and mortality. (A–D) Age-dependent survival with median (50%) and maximum (90%) life span in days indicated and (E–H) mortality risk ($\mu(x)$) estimated from the best-fitting models for each species (Table S1) in BaSTA. Red, dry region; blue, wet region. Survival plots were produced using a Kaplan–Maier estimator (*survival* package).

Table 2. Population-specific estimates of mortality parameters and their SEs.

Species	Region	*N*	Best model	IMR[1] ± SE	KL[2]	RoA[3] ± SE	KL	*s*[4] ± SE	KL
N. furzeri	Dry	79	Logistic simple	−3.77 ± 0.37	0.50	0.370 ± 0.090	0.71	1.52 ± 0.53	0.82
N. furzeri	Wet	80		−3.81 ± 0.37		0.287 ± 0.076		2.36 ± 0.65	
N. kadleci	Dry	73	Weibull simple	1.30 ± 0.12	0.96	0.056 ± 0.006	0.99		
N. kadleci	Wet	75		1.60 ± 0.14		0.042 ± 0.003			
N. orthonotus	Dry	99	Weibull simple	1.42 ± 0.12	0.57	0.040 ± 0.003	0.54		
N. orthonotus	Wet	101		1.36 ± 0.11		0.041 ± 0.003			
N. pienaari	Dry	113	Weibull bathtub	3.32 ± 0.55	0.81	0.023 ± 0.002	0.87		
N. pienaari	Wet	103		2.63 ± 0.48		0.020 ± 0.002			

For selected best-fitting aging models for each species, see Figure 1.

[1]IMR, initial mortality rate (baseline, age-independent mortality).

[2]KL, Kullback–Leibler discrepancy criterion overlap in posterior parameter estimates between two populations (0.5—complete overlap, 1.0—no overlap).

[3]RoA, rate of aging (increase in mortality with age, the measure of aging rate).

[4]*s*, mortality deceleration rate (in logistic model).

$P = 0.078$), with a slightly steeper decline (interaction: $z = 2.49$, $P = 0.013$). A decline in relative clutch size was evident in *N. kadleci*, *N. orthonotus*, and *N. pienaari* (Fig. 3C and Table S8).

Fertilization rate decreased with age (binomial GLMM: $z = 10.40$, $P < 0.001$, $n = 522$) and a stronger decline was recorded in the dry-region populations (age by region interaction: $z = 4.57$, $P < 0.001$, Fig. 3D), providing clear evidence of reproductive aging. Dry-region populations tended to have lower fertilization success overall ($z = 1.83$, $P = 0.067$). Decline with age was strongest in *N. orthonotus* and absent in *N. furzeri* (Fig. 3D and Table S8).

Egg size increased significantly with age (LMM, age: $t_{2763} = 3.31$, $P = 0.001$, Fig. 2E), but did not differ between regions (region: $t_5 = 0.06$, $P = 0.955$; age by region interaction: $t_{3613} = 1.78$, $P = 0.075$), regardless of whether female and clutch sizes were included in the model (Table S8). Egg size increase with age was strongest in *N. orthonotus*, but absent in *N. kadleci* (Fig. 3E), positively related to female size and negatively associated with clutch size (Table S8).

LIFE-HISTORY TRAITS AND PACE-OF-LIFE SYNDROME

High interspecific variability resulted in no general support for predictions on rapid early development in dry-region populations. Overall, hatching size (LMM: $t_3 = 0.78$, $P = 0.493$, Fig. 2G), size at sexual maturity ($t_3 = 0.62$, $P = 0.584$), time to maturity ($t_3 = 1.00$, $P = 0.390$), and maximum body size (males: $t_{2.04} = 0.47$, $P = 0.684$; females: $t_{2.04} = 0.46$, $P = 0.688$) did not differ between regions. The best support for predictions was demonstrated in *N. pienaari*, with larger body size at hatching translating into earlier onset of sexual maturity at a larger size in the dry-region population. Earlier maturity was also attained by dry-region *N. kadleci*, despite their smaller size at hatching. In contrast, mixed evidence for more rapid early life history was demonstrated in dry-region *N. orthonotus* and no interpopulation contrasts were found in *N. furzeri* (Fig. 4A–C and Table S9). Maximum adult size did not differ intraspecifically (Fig. 4D).

No behavioral or metabolic trait associated with "pace-of-life syndrome" differed between dry- and wet-region populations. Overall, there was no significant difference in RMR (LMM: $t_{1.83} = 0.49$, $P = 0.676$), maximum metabolic rate ($t_1 = 0.40$, $P = 0.691$), and MS ($t_1 = 0.09$, $P = 0.943$, n = 66), as well as no difference in individual boldness (emergence from a refuge; mixed-effect Cox model: $z = 0.20$, $P = 0.840$, $n = 313$), aggression (attacks on a rival male; LMM: $t_{99} = 0.37$, $P = 0.91$), and exploratory activity (distance traveled in novel environment; *N. furzeri* and *N. kadleci*, LMM: $t_{120.4} = 0.63$, $P = 0.528$ and *N. orthonotus* and *N. pienaari*, LMM: $t_{69.7} = 0.64$, $P = 0.523$). The analyses for separate species were consistent with the results for general outcome (Fig. 5 and Tables S9 and S10).

Discussion

Using annual fishes from ephemeral pools on the African savannah, we followed almost 1000 individuals from eight populations and demonstrated aging at demographic, functional, and reproductive levels. We showed that intraspecific patterns of aging matched predictions of the evolutionary theory of aging; populations from drier regions (with shorter life expectancy) had shorter life spans. Notably, shorter life spans were related to a faster increase in mortality risk with age rather than differences in baseline mortality. Demographic differences in life span and aging among populations were coupled with functional and reproductive declines. In contrast, our data did not provide support for the evolution of divergent early life history (rapid growth and maturation) and pace-of-life syndrome (higher metabolic rate,

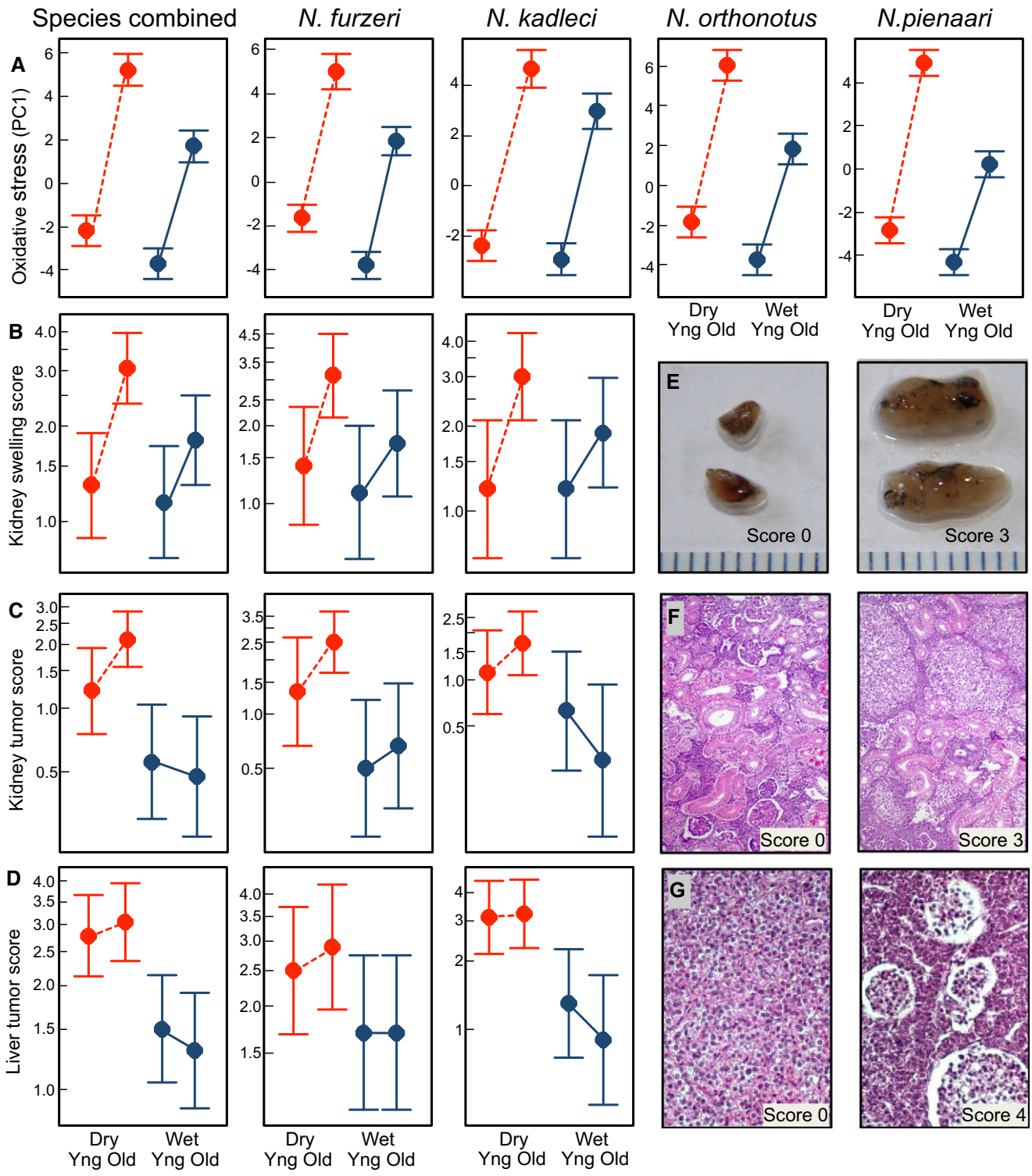

Figure 2. Functional aging between dry- and wet-region populations and examples of histopathologies. Contrasts in estimates of oxidative stress (A), cephalic kidney swelling (B), cephalic kidney tumors (C), and liver tumors (D) of populations from dry (red, broken line) and wet (blue, solid line) regions in young and old fish for all species pooled and for separate species. Values represent mean and 95% confidence intervals from model estimates (R package *effects*). Results of species-specific analyses are given in Table S7. Illustration of normal and swollen cephalic kidney (E, scale bar 1 mm), histological section of healthy and tumor-burdened cephalic kidney (F), and histological section of healthy liver and tumor-burdened liver (G).

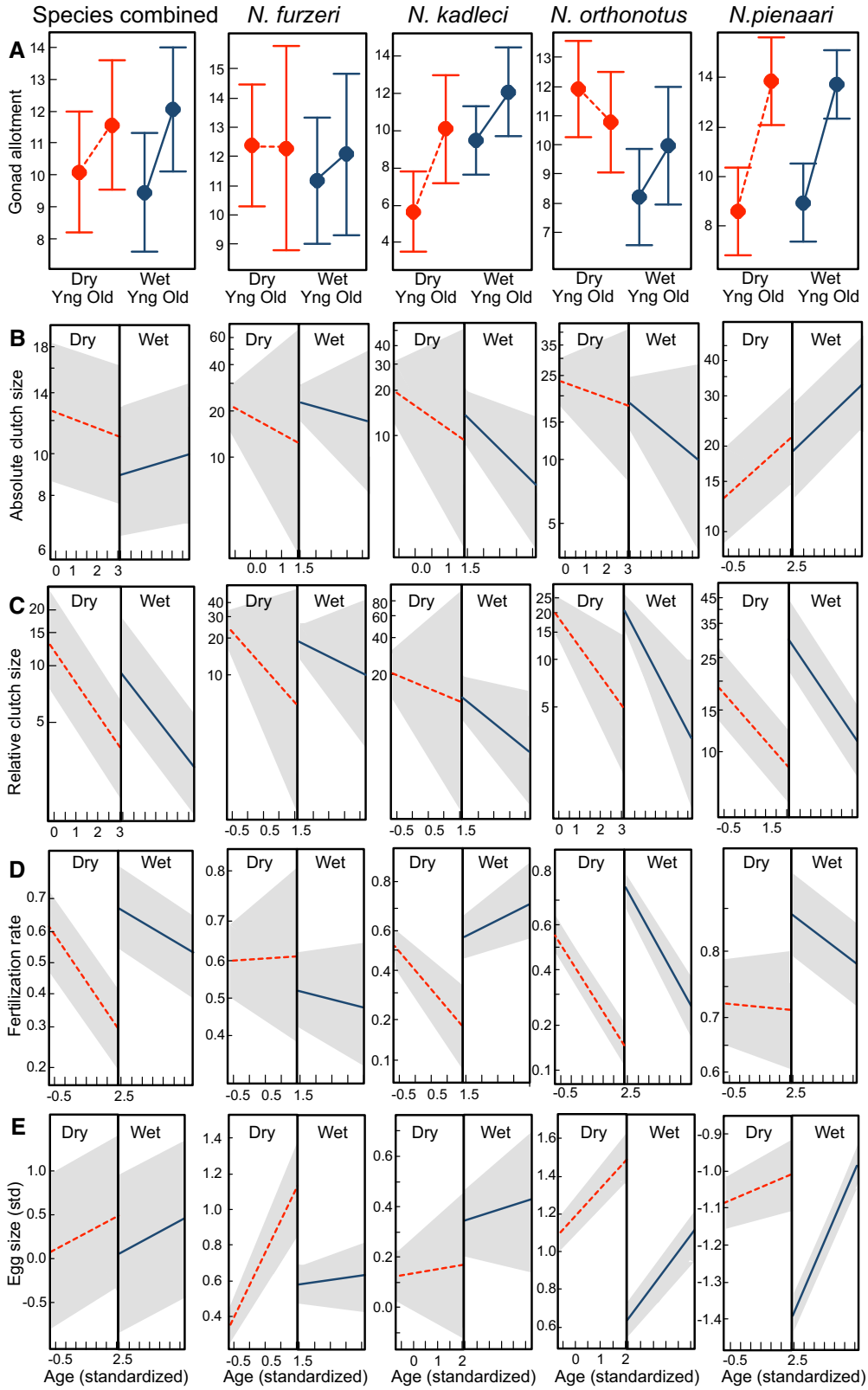

Figure 3. Reproductive aging in dry-region (red, broken line) and wet-region (blue, solid line) populations. Contrasts in estimates of gonad allotment (GSIt) in young and old females (A), and absolute clutch size (B), relative clutch size (C), fertilization rate (D), and egg size (E) measured at 10-week intervals. Estimates for all species combined and for separate species are given. Values represent mean and 95% confidence intervals from model estimates (R package *effects*). Results of species-specific analyses are given in Table S8.

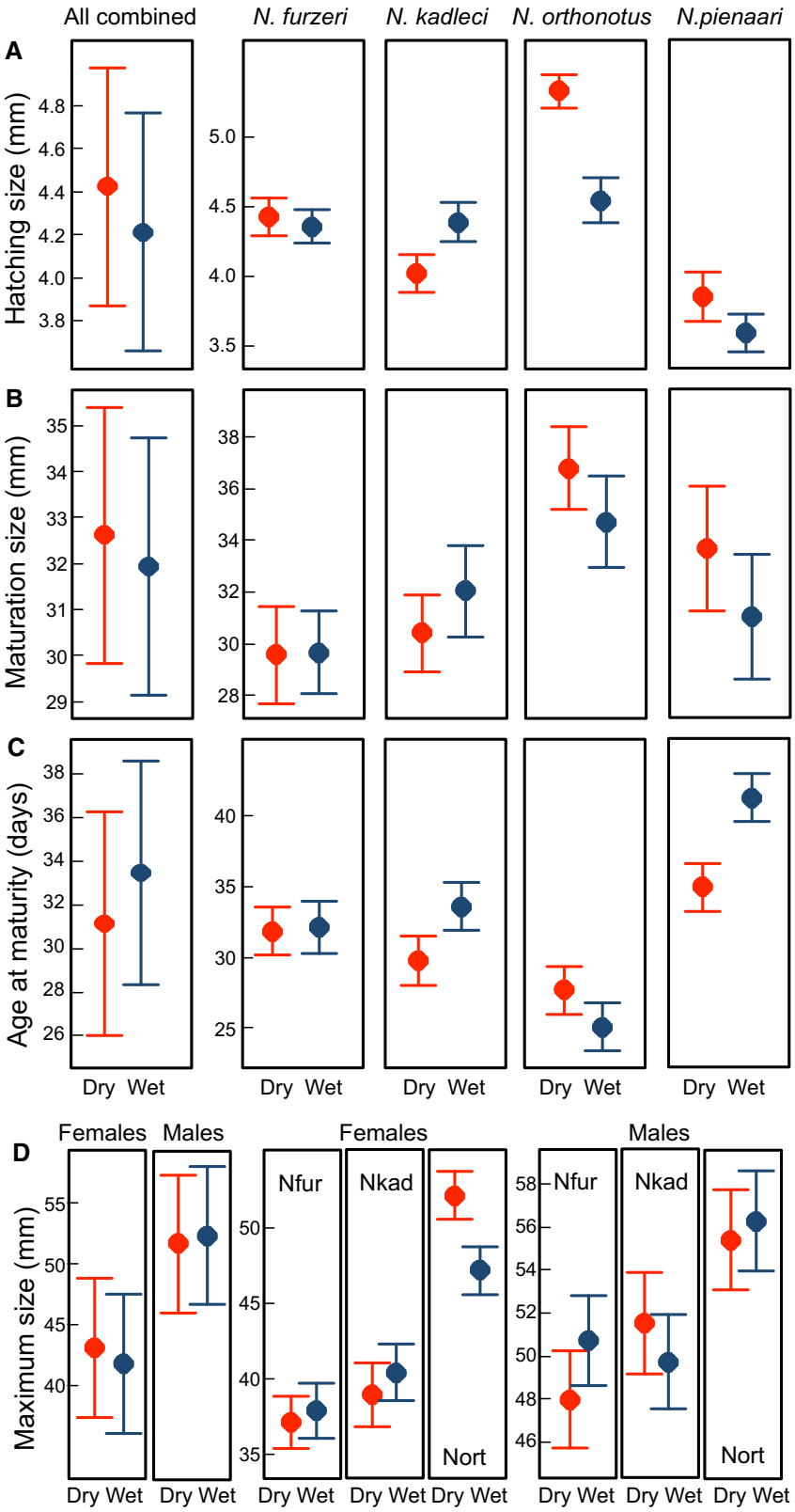

Figure 4. Life-history traits of dry- and wet-region populations. Contrasts in hatching size (A), size at sexual maturity (B), age at sexual maturity (C), and maximum body size (D) of populations from dry (red) and wet (blue,) regions for all species pooled and for separate species. Values represent mean and 95% confidence intervals from model estimates (R package *effects*). Results of species-specific analyses are given in Table S9. Nfur, *Nothobranchius furzeri*; Nkad, *Nothobranchius kadleci*; Nort, *Nothobranchius orthonotus*; Npie, *Nothobranchius pienaari*.

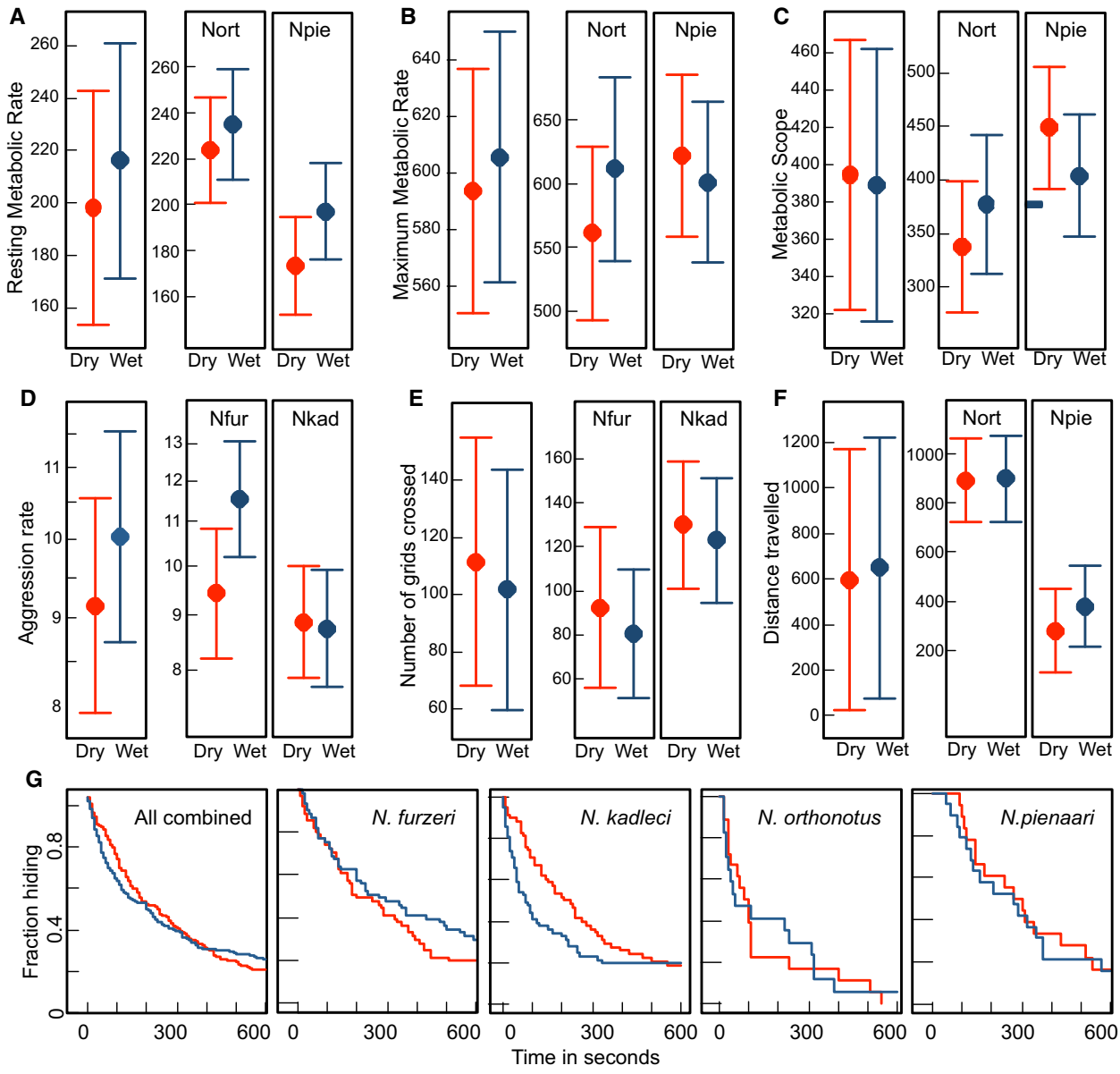

Figure 5. **Pace-of-life syndrome traits from dry- and wet-region populations. Contrasts in resting metabolic rate (A), maximum metabolic rate (B), metabolic scope (C), aggression rate (D), activity level expressed as the number of grids crossed during 4 min (E, two species) and total distance traveled over 4 min (F, two species) and estimates of emergence from a refuge (G) for populations from dry (red) and wet (blue) regions for all species combined and for separate species. Values represent mean and 95% confidence intervals from model estimates (R package *effects*). Emergence is visualized as fraction of hiding fish (package *survival*). Results of species-specific analyses are given in Tables S9 and S10. Nfur, *Nothobranchius furzeri*; Nkad, *Nothobranchius kadleci*; Nort, *Nothobranchius orthonotus*; Npie, *Nothobranchius pienaari*.**

more active behavior) associated with life span and aging differences at the interpopulation level.

Within species, the predicted positive relationship between extrinsic mortality and life span may be complicated by a strong link between individual condition and survival (Reznick et al. 2004; Chen and Maklakov 2012; Hämäläinen et al. 2014). However, life span (longevity) is not necessarily correlated with aging (i.e., with an increase in mortality with age) and functional and reproductive deterioration (Baudisch 2011; Reichard 2016). For example, laboratory experiments on wild-derived guppies revealed that populations with high predation risk evolved longer (rather than shorter) life spans than populations with low predation risk (Reznick et al. 2004). However, longer lived guppy populations from high-predation environments actually had a higher rate of

increase in mortality rate with age (i.e., RoA, parameter γ in a Gompertz model) and their longer life span apparently was a consequence of a lower baseline mortality (Reznick et al. 2004: their Table S3). In addition, guppies from high mortality risk populations demonstrated greater functional deterioration in terms of escape response (Reznick et al. 2004), in accordance with standard predictions. The high-predation guppy populations, therefore, may have evolved longer life spans but, arguably, faster aging rates. This conclusion suggests that condition-dependent survival may select for longer life span by decreasing baseline mortality rates rather than slowing the increase of mortality with age. Most importantly, it implies that interpretation of the evolutionary patterns of aging depends on how aging is defined (Bronikowski and Promislow 2005). Overall, this underscores the importance of functional assays to identify aging-related deterioration in benign captive environments.

Functional deterioration in killifish, measured in terms of an increase in oxidative damage and tumor-associated pathologies in the liver and cephalic kidney, was unambiguously higher in dry-region populations. Age-related declines were most apparent in oxidative stress and kidney pathologies also tended to deteriorate with age. Tumor load in the liver did not increase with age and we speculate that high tumor load in young fish from dry-region populations may have increased individual mortality early in life, producing the apparent lack of increase in tumor load with age as individuals with high tumor load did not survive to sampling at older ages. We have focused on a comparison between populations in this study but future analyses should investigate the relationship between individual measures of functional declines and individual-based estimates of phenotypic traits collected prior to aging marker assays. Such an analysis can reveal condition-dependent survival at the individual (intrapopulation) level, trade-offs between reproductive effort and senescence, and patterns of synchrony and correlation between specific individual declines (Gavrilov and Gavrilova 2001; Massot et al. 2011; Bouwhuis et al. 2012; Hayward et al. 2015; Dong et al. 2016). We acknowledge that our study was not aimed at, and cannot provide any conclusion on, the causal relationships behind mortality patterns. This was an inevitable outcome of our study design because sacrificing of individuals was required for tissue sampling; nondestructive histological sampling is not feasible in our study taxon.

Reproductive aging is commonly assumed to be rare in fish (Reznick et al. 2002; Kishi et al. 2003). Fish possess the capacity to substantially increase fecundity with age because growth is typically indeterminate and body mass and fecundity are strongly positively correlated (Wootton and Smith 2015). Nonetheless, unambiguous reproductive aging was reported in captive guppies, including a relatively extended postreproductive life span (Reznick et al. 2006), and decline in fertility with age is commonly recognized in freshwater fish aquaculture, where old fish are purposely removed from breeding programs. We demonstrated reproductive aging primarily in relative (i.e., size-corrected) clutch size and fertilization rate, with stronger declines in dry-region populations. The absolute clutch size (i.e., uncorrected for body size) also decreased in many populations, though it increased in both populations of the longest lived species *N. pienaari*. Relative gonad mass increased rather than decreased in older females. The degree of reproductive declines varied across species. No reproductive aging was detected in the shortest lived *N. furzeri*, with no evidence even of a decline in fertilization rate with age. This finding could, however, be an artifact of the experimental design; our 10-week sampling intervals were possibly too long to capture terminal reproductive declines associated with rapid *N. furzeri* mortality between 20 and 30 weeks of age. In *Nothobranchius* fishes, histopathological analysis revealed fibrosis, degeneration, and atrophy in various combinations and degrees in testes and follicular degeneration, fibrosis, and severe neoplastic formation in females (di Cicco et al. 2011). Although we have not included an analysis of the histopathology of the gonads in the present study, it is likely that declines in fertilization rate were related to histological changes in the gonads.

Life span and aging rates coevolve with other life-history traits. Our data provided only limited support for the relationship between short life span (and rapid aging) and rapid maturation (Stearns 1992). We predicted larger body size at hatching in dry-region populations, but confirmed the relationship only in two species (*N. orthonotus* and *N. pienaari*), whereas the reverse pattern was found in *N. kadleci*. In accordance with the predictions, it took the dry-region *N. kadleci* and *N. pienaari* six and three days shorter, respectively, to reach sexual maturity than their wet-region conspecifics, though dry-region *N. orthonotus* matured two days later than their wet-region conspecifics. Along with an absence of interpopulation differences in juvenile development in *N. furzeri*, this finding demonstrates a complex pattern of early life history among Mozambican *Nothobranchius* species and populations that was not consistent with our hypothesis of concerted evolution of aging and life history. We acknowledge that multiple populations from each region and each species would be ultimately required to provide a fuller understanding of life-history evolution along the gradient of aridity.

Pace-of-life syndrome can evolve at the interpopulation level, when rapid life history is associated with high metabolic rate (Wikelski et al. 2003) and more active and risky behavior (Reále et al. 2010). However, we found no support for pace-of-life syndrome at the interpopulation level in any trait. Divergent selection acting on *Nothobranchius* population-level life histories in dry and wet regions stems primarily from a temporal axis of habitat deterioration; diet, predation risk, habitat size, and complexity, water quality and temperature are similar across the region, but

highly variable within and among generations (Reichard et al. 2009; Polačik et al. 2014b; Reichard et al. 2014; Reichard 2015). A possibility is that only more complex and predictable niche divergence (such as alternative ecotypes associated with different developmental conditions, ecological settings or migratory behavior) generates distinct population-level pace-of-life syndromes (Wikelski et al. 2003; Bronikowski and Vleck 2010).

In our study, we focused on contrasts in aging rates and associated phenotypic traits between populations with short and long life expectancy. We primarily treated species as metareplicates to provide robust understanding of the evolution of aging and life-history traits of annual fish populations across an environmental gradient. Species-specific details in dry–wet region contrasts suggest a combination of traits that conform with or contradict theoretical predictions. For example, no difference in life span and demographic aging was detected between *N. orthonotus* populations, though the populations differed in functional and reproductive aging in the predicted direction. In general, the differences were strongest in *N. pienaari* and *N. orthonotus*, two species with ranges that provided the largest contrasts along the aridity gradient and with the longest life spans. Aging is multifarious process (Gavrilov and Gavrilova 2001)—asymmetry and asynchrony in specific declines, within and among individuals (Hayward et al. 2015; Dong et al. 2016), along with condition-dependent survival can produce the observed mosaic of aging at the interpopulation level. The apparent lack of an evolutionary response to selection for more rapid life history in dry-region populations may stem from developmental constraints; *N. furzeri* and *N. kadleci* are species with the shortest maturation time recorded in any vertebrates (Blažek et al. 2013) and further shortening of the juvenile period may not be biologically feasible for a vertebrate.

In conclusion, our findings imply that the shorter existence of temporary pools in the dry region repeatedly selected for shorter life span and more rapid demographic, functional, and reproductive aging in African annual fishes. This parallel intraspecific divergence in life span and aging was not associated with divergence in early life history, behavior, or metabolic traits. Future research should use longitudinal data to link early life history, life span, and functional deterioration at the individual level. Such a study would broaden our understanding of causal relationships behind observed mortality patterns and provide functional insights into individual variation in life span.

ACKNOWLEDGMENTS

We thank C. Smith, F. Colchero, R. Spence, P. Morais and two anonymous referees for valuable comments. Funding came from Czech Science Foundation (13-05872S and 16–00291S) to MR. PK acknowledges support from the Operational Programme Prague—Competitiveness (CZ.2.16/3.1.00/22197) and National Program of Sustainability (NPU I LO1215; MSMT—34870/2013). AC was supported by Scuola Normale Superiore (CELSNS2015). All work was approved by the ethical committees of the Institute of Vertebrate Biology (No. 163-12) and the Ministry of Agriculture (CZ 62760203) and complies with the legal regulations of the Czech Republic. RB completed the main experiment with the assistance of MP and MV; PK, KS, OT, TA analyzed oxidative stress; RŘ completed behavioral assays; CM measured metabolism; AC, ETT, and RB performed histological assays; MR conceived and designed the study, conducted statistical analyses, and wrote the manuscript. All authors contributed to the final text. We declare to have no conflict of interest.

DATA ARCHIVING

Data available from the Dryad Digital Repository: http://dx.doi.org/10.5061/dryad.4gv4g.

LITERATURE CITED

Austad, S. N. 1993. Retarded senescence in an insular population of Virginia opossums (*Didelphis virginiana*). J. Zool. 229:695–708.

Bartáková, V., M. Reichard, K. Janko, M. Polačik, R. Blažek, K. Reichwald, A. Cellerino, and J. Bryja. 2013. Strong population genetic structuring in an annual fish, *Nothobranchius furzeri*, suggests multiple savannah refugia in southern Mozambique. BMC Evol. Biol. 13:1–15.

Bartáková, V., M. Reichard, R. Blažek, M. Polačik, and J. Bryja. 2015. Terrestrial fishes: rivers are barriers to gene flow in annual fishes from the African savanna. J. Biogeogr. 42:1832–1844.

Bates, D., M. Maechler, B. Bolker, and S. Walker. 2014. Lme4: linear mixed-effects models using Eigen and S4. R package 1.1-6. Available at http://CRAN.R-project.org/package=lme4.

Baudisch, A. 2011. The pace and shape of ageing. Meth. Ecol. Evol. 2:375–382.

Baumgart, M., E. Di Cicco, G. Rossi, A. Cellerino, and E. T. Tozzini. 2015. Comparison of captive lifespan, age-associated liver neoplasias and age-dependent gene expression between two annual fish species: *Nothobranchius furzeri* and *Nothobranchius korthause*. Biogerontology 16:63–69.

Blažek, R., M. Polačik, and. M. Reichard. 2013. Rapid growth, early maturation and short generation time in African annual fishes. EvoDevo 4:1–7.

Blumstein, D. T., and J. C. Daniel. 2007. Quantifying behavior: the JWatcher Way. Sinauer Associates, Sunderland.

Bouwhuis, S., R. Choquet, B. C. Sheldon, and S. Verhulst. 2012. The forms and fitness cost of senescence: age-specific recapture, survival, reproduction, and reproductive value in a wild bird population. Am. Nat. 179:E15–E27.

Bronikowski, A. M., and D. E. Promislow. 2005. Testing evolutionary theories of aging in wild populations. Trends Ecol. Evol. 20:271–273.

Bronikowski, A. M., and D. Vleck 2010. Metabolism, body size and life span: a case study in evolutionarily divergent populations of the garter snake (*Thamnophis elegans*). Integr. Comp. Biol. 50:880–887.

Bronikowski, A. M., S. C. Alberts, J. Altmann, C. Packer, K. D. Carey, and M. Tatar. 2002. The aging baboon: comparative demography in a non-human primate. Proc. Natl. Acad. Sci. USA 99:9591–9595.

Brown, C., and V. A. Braithwaite. 2004. Size matters: a test of boldness in eight populations of the poeciliid *Brachyraphis episcopi*. Anim. Behav. 68:1325–1329.

Brown, D. 2009. Tracker video analysis and modeling tool (version 4.82). Available at http://www.cabrillo.edu/˜dbrown/tracker/ (accessed September 22, 2015).

Cellerino, A., D. R. Valenzano, and M. Reichard. 2016. From the bush to the bench: the annual *Nothobranchius* fishes as a new model system in biology. Biol. Rev. 91:511–533.

Chen, H. Y., and A. A. Maklakov. 2012. Longer life span evolves under high rates of condition-dependent mortality. Curr. Biol. 22:2140–2143.

Chen, H. Y., F. Zajitschek, and A. A. Maklakov. 2013. Why ageing stops: heterogeneity explains late-life mortality deceleration in nematodes. Biol. Lett. 9:20130217.

Clarke, A., and N. M. Johnston. 1999. Scaling of metabolic rate with body mass and temperature in teleost fish. J. Anim. Ecol. 68:893–905.

Colchero, F., O. R. Jones, and M. Rebke. 2012. BaSTA: an R package for Bayesian estimation of age-specific survival from incomplete mark–recapture/recovery data with covariates. Methods Ecol. Evol. 3:466–470.

Di Cicco, E., E. T. Tozzini, G. Rossi, and A. Cellerino. 2011. The short-lived annual fish *Nothobranchius furzeri* shows a typical teleost aging process reinforced by high incidence of age-dependent neoplasias. Exp. Gerontol. 46:249–256.

Dong, Y., P. Cui, Z. Li, and S. Zhang. 2016. Aging asymmetry: systematic survey of changes in age-related biomarkers in the annual fish *Nothobranchius guentheri*. Fish Physiol. Biochem. DOI:10.1007/s10695-016-0288-1.

Dudycha, J. L., and A. J. Tessier. 1999. Natural genetic variation of life span, reproduction, and juvenile growth in *Daphnia*. Evolution 53:1744–1756.

Fontana, L., B. K. Kennedy, V. D. Longo, D. Seals, and S. Melov. 2014. Medical research: treat ageing. Nature 511:405–407.

Gavrilov, L. A., and N. S. Gavrilova. 2001. The reliability theory of aging and longevity. J. Theor. Biol. 213:527–545.

Hämäläinen, A., M. Dammhahn, F. Aujard, M. Eberle, I. Hardy, P. M. Kappeler, M. Perret, S. Schliehe-Diecks, and C. Kraus. 2014. Senescence or selective disappearance? Age trajectories of body mass in wild and captive populations of a small-bodied primate. Proc. R. Soc. Lond. B Biol. Sci. 281:20140830.

Hayward, A. D., A. J. Wilson, J. G. Pilkington, T. H. Clutton-Brock, J. M. Pemberton, and L. E. Kruuk. 2013. Reproductive senescence in female Soay sheep: variation across traits and contributions of individual ageing and selective disappearance. Funct. Ecol. 27:184–195.

Hayward, A. D., J. Moorad, C. E. Regan, C. Berenos, J. G. Pilkington, J. M. Pemberton, and D. H. Nussey. 2015. Asynchrony of senescence among phenotypic traits in a wild mammal population. Exp. Gerontol. 71:56–68.

Jones, O. R., J. M. Gaillard, S. Tuljapunkar, J. S. Alho, K. B. Armitage, P. H. Becker, P. Bize, J. Brommer, A. Charmantier, T. Clutton-Brock, et al. 2008. Senescence rates are determined by ranking on the fast–slow life-history continuum. Ecol. Lett. 11:664–673.

Kirkwood, T. B., and S. N. Austad. 2000. Why do we age? Nature 408:233–238.

Kirkwood, T. L. 1977. Evolution of ageing. Nature 270:301–304.

Kishi, S., J. Uchiyama, A. M. Baughman, T. Goto, M. C. Lin, and S. B. Tsai. 2003. The zebrafish as a vertebrate model of functional aging and very gradual senescence. Exp. Gerontol. 38:777–786.

Kraus, C., S. Pavard, and D. E. Promislow. 2013. The size–life span trade-off decomposed: why large dogs die young. Am. Nat. 181:492–505.

Larson, S. M., F. Colchero, O. R. Jones, L. Williams, and E. Fernandez-Duque. 2016. Age and sex-specific mortality of wild and captive populations of a monogamous pair-bonded primate (*Aotus azarae*). Am. J. Primatol. 78:315–325.

Lohr, J. N., P. David, and C. R. Haag. 2014. Reduced lifespan and increased ageing driven by genetic drift in small populations. Evolution 68:2494–2508.

López-Otín, C., M. A. Blasco, L. Partridge, M. Serrano, and G. Kroemer. 2013. The hallmarks of aging. Cell 153:1194–1217.

Maklakov, A. A., L. Rowe, and U. Friberg. 2015. Why organisms age: evolution of senescence under positive pleiotropy? Bioessays 37:802–807.

Massot, M., J. Clobert, L. Montes-Poloni, C. Haussy, J. Cubo, and S. Meylan. 2011. An integrative study of ageing in a wild population of common lizards. Funct. Ecol. 25:848–858.

Medawar, P. B. 1952. An unsolved problem of biology. H. K. Lewis, London.

Monaghan, P., N. B. Metcalfe, and R. Torres. 2009. Oxidative stress as a mediator of life history trade-offs: mechanisms, measurements and interpretation. Ecol. Lett. 12:75–92.

Pamplona, R., and D. Costantini. 2011. Molecular and structural antioxidant defenses against oxidative stress in animals. Am. J. Physiol. Regul. Integr. Comp. Physiol. 301:R843–R863.

Pletcher, S. D. 1999. Model fitting and hypothesis testing for age-specific mortality data. J. Evol. Biol. 12:314–328.

Pletcher, S. D., A. A. Khazaeli, and J. W. Curtsinger. 2000. Why do life spans differ? Partitioning mean longevity differences in terms of age-specific mortality parameters. J. Gerontol. A Biol. Sci. Med. Sci. 55:B381–B389.

Polačik, M., and M. Reichard. 2009. Indirect fitness benefits are not related to male dominance in a killifish. Behav. Ecol. Sociobiol. 63:1427–1435.

———. 2011. Asymmetric reproductive isolation between two sympatric annual killifish with extremely short lifespans. PLoS ONE 6:e22684.

Polačik, M., M. T. Donner, and M. Reichard. 2011. Age structure of annual *Nothobranchius* fishes in Mozambique: is there a hatching synchrony? J. Fish Biol. 78:796–809.

Polačik, M., R. Blažek, R. Řežucha, M. Vrtílek, E. Terzibasi Tozzini, and M. Reichard. 2014a. Alternative intrapopulation life-history strategies and their trade-offs in an African annual fish. J. Evol. Biol. 27:854–865.

Polačik, M., C. Harrod, R. Blažek, and M. Reichard. 2014b. Trophic niche partitioning in communities of African annual fish: evidence from stable isotopes. Hydrobiologia 721:99–106.

Polačik, M., R. Blažek, and M. Reichard. 2016. Laboratory breeding of the short-lived annual killifish *Nothobranchius furzeri*. Nat. Protoc. 11:1396–1413.

Réale, D., D. Garant, M. M. Humphries, P. Bergeron, V. Careau, and P. O. Montiglio. 2010. Personality and the emergence of the pace-of-life syndrome concept at the population level. Philos. Trans. R. Soc. Lond. B Biol. Sci. 365:4051–4063.

Reichard, M. 2015. The evolutionary ecology of African annual fishes. Pp. 133-158 *in* N. Berois, G. García, and R. de Sá, eds. Annual fishes: life history strategy, diversity, and evolution. CRC Press, Boca Raton, FL.

———. 2016. Evolutionary ecology of ageing: time to reconcile field and laboratory research. Ecol. Evol. 6:2988–3000.

Reichard, M., M. Polačik, and O. Sedláček. 2009. Distribution, colour polymorphism and habitat use of the African killifish *Nothobranchius furzeri*, the vertebrate with the shortest life span. J. Fish Biol. 74:198–212.

Reichard, M., M. Polačik, R. Blažek, and M. Vrtílek. 2014. Female bias in the adult sex ratio of African annual fishes: interspecific differences, seasonal trends and environmental predictors. Evol. Ecol. 28:1105–1120.

Reuter, S., S. C. Gupta, M. M. Chaturvedi, and B. B. Aggarwal. 2010. Oxidative stress, inflammation, and cancer: how are they linked? Free Radic. Biol. Med. 49:1603–1616.

Reznick, D., C. Ghalambor, and L. Nunney. 2002. The evolution of senescence in fish. Mech. Ageing Dev. 123:773–789.

Reznick, D., M. Bryant, and D. Holmes. 2006. The evolution of senescence and post-reproductive lifespan in guppies (*Poecilia reticulata*). PLoS Biol. 4:e7.

Reznick, D. N., M. J. Bryant, D. Roff, C. K. Ghalambor, and D. E. Ghalambor. 2004. Effect of extrinsic mortality on the evolution of senescence in guppies. Nature 431:1095–1099.

Ricklefs, R. E. 2010. Insights from comparative analyses of aging in birds and mammals. Aging Cell 9:273–284.

Ricklefs, R. E., and M. Wikelski. 2002. The physiology/life-history nexus. Trends Ecol. Evol. 17:462–468.

Rose, M. R. 1994. Evolutionary biology of aging. Oxford Univ. Press, Oxford, U.K.

Stearns, S. C. 1992. The evolution of life histories. Oxford Univ. Press, Oxford, U.K.

Stearns, S. C., M. Ackermann, M. Doebeli, and M. Kaiser. 2000. Experimental evolution of aging, growth, and reproduction in fruit flies. Proc. Natl. Acad. Sci. USA 97:3309–3313.

Steffensen, J. F. 1989. Some errors in respirometry of aquatic breathers: how to avoid and correct for them. Fish Physiol. Biochem. 6:49–59.

Syslová, K., A. Böhmová, M. Mikoška, M. Kuzma, D. Pelclová, and P. Kačer. 2014. Multimarker screening of oxidative stress in aging. Oxid. Med. Cell. Longev. Article ID 562860.

Tatar, M., D. W. Gray, and J. R. Carey. 1997. Altitudinal variation for senescence in *Melanoplus* grasshoppers. Oecologia 111:357–364.

Terzibasi Tozzini, E., A. Dorn, E. Ng'oma, M. Polačik, R. Blažek, K. Reichwald, A. Petzold, B. Watters, M. Reichard, and A. Cellerino. 2013. Parallel evolution of senescence in annual fishes in response to extrinsic mortality. BMC Evol. Biol. 13:77.

Therneau, T. M. 2015a. Mixed effects Cox models. R package version 2.2-5. Available at http://CRAN.R-project.org/package=coxme.

———. 2015b. Survival analysis. R package version 2.38-3. Available at http://CRAN.R-project.org/package=survival.

Vaupel, J. W., and A. I. Yashin. 1985. Heterogeneity's ruses: some surprising effects of selection on population dynamics. Am. Stat. 39:176–185.

Vrtílek, M., and M. Reichard. 2015. Highly plastic resource allocation to growth and reproduction in females of an African annual fish. Ecol. Freshw. Fish 24:616–628.

———. 2016. Female fecundity traits in wild populations of African annual fish: the role of the aridity gradient. Ecol. Evol. 6:5921–5931.

Wikelski, M., L. Spinney, W. Schelsky, A. Scheuerlein, and E. Gwinner. 2003. Slow pace of life in tropical sedentary birds: a common-garden experiment on four stonechat populations from different latitudes. Proc. R. Soc. Lond. B Biol. Sci. 270:2383–2388.

Williams, G. C. 1957. Pleiotropy, natural selection, and the evolution of senescence. Evolution 11:398–411.

Williams, P. D., and T. Day. 2003. Antagonistic pleiotropy, mortality source interactions, and the evolutionary theory of senescence. Evolution 57:1478–1488.

Williams, P. D., T. Day, Q. Fletcher, and L. Rowe. 2006. The shaping of senescence in the wild. Trends Ecol. Evol. 21:458–463.

Wootton, R. J., and C. Smith. 2015. Reproductive biology of teleost fishes. Wiley-Blackwell, Chichester.

Associate Editor: T. Flatt
Handling Editor: P. Tiffin

Supporting Information

Additional Supporting Information may be found in the online version of this article at the publisher's website:

Figure S1. Map of southern and central Mozambique with annual precipitation totals and collections sites of the source study populations.
Figure S2. Liver tumors and kidney tumor-associated swelling.
Figure S3. Posterior distributions of model parameters for the best fitting models for each species.
Figure S4. Posterior distributions of model parameters for the logistic model constructed for all populations pooled.
Table S1. Relative fit of demographic models of ageing in BaSTA ranked on the basis of difference in DIC (Deviance Information Criterion).
Table S2. Age, relative survival and sample size for fish taken for analyses of functional ageing (left) and pace-of-life syndrome (right).
Table S3. The validation parameters of LC-MS methods for determination of biomarkers of oxidative stress.
Table S4. Principal Component Analysis combining oxidative stress in liver, brain and heart using biomarkers of damage to lipids, proteins and DNA.
Table S5. Population-specific estimates of mortality parameters from logistic model and their standard errors.
Table S6. Results from General Linear Models from organ-specific and biomarker-specific analyses of oxidative damage.
Table S7. Linear model results from species-specific analyses of oxidative damage (PC1, details in Table S4) and histopathological declines.
Table S8. Results of species-specific analyses of reproductive ageing.
Table S9. Results of species-specific analyses of life history and behavioral traits, with interpretation of significant results.
Table S10. Results of overall (General Linear Models, random effect *Population* nested within *Species*) and species-specific (Linear Models) analyses of metabolic traits, with interpretation of significant results.